JOC Article

Molecular Dynamics and Docking Studies of Single Site Esterase Peptide Dendrimers

Sacha Javor and Jean-Louis Reymond*

Department of Chemistry and Biochemistry, University of Berne, Freiestrasse 3, CH-3012, Berne, Switzerland

jean-louis.reymond@ioc.unibe.ch

Received December 16, 2008

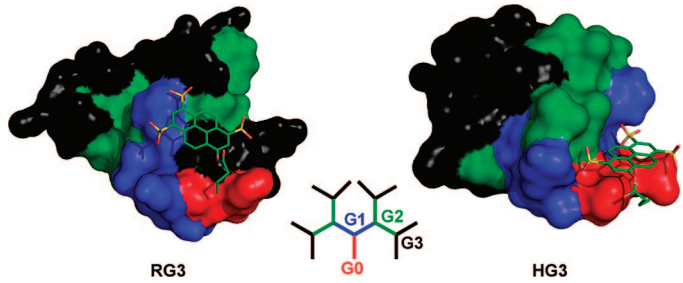

Herein we report the first molecular dynamics and docking study of peptide dendrimers, at the example of dendrimers catalyzing the hydrolysis of acyloxy pyrene trisulfonates in aqueous buffer. Molecular dynamics provide models comparable to the observation by diffusion-NMR showing that the dendrimers exist as conformationally flexible molten globules in aqueous solution. Packing is evidenced by the occurrence of close contacts between topologically distant amino acids in the dendrimer model. Backbone hydrogen bonds predominantly form 2, 3, or 4 residues apart as found in the secondary structures of proteins, however, with lower frequency. The catalytic residues are present at the surface of the dendrimer model at relative positions compatible with binding and esterolysis. Docking of the substrate to low-energy conformations of the dendrimers predicts the formation of dendrimer−substrate complexes with one or two salt bridges between the sulfonate and protonated arginine or histidine residues. Substrate binding in the docked models also involves 4−6 van der Waals contacts. In the catalytic dendrimers **RG3** and **RMG3** exhibiting a positive dendritic effect, these docking contacts involve the outer dendritic branches. By contrast, in the catalytic dendrimers **HG3** or **HMG3** where no such effect occurs, the docking contacts are concentrated at the dendritic core. The present investigations provide an unprecedented insight into the molecular dynamics of peptide dendrimers that may be of general significance for other conformationally flexible dendrimers.

Introduction

Dendrimers are branched synthetic macromolecules adopting a globular or disk-shaped conformation as a result of their topology.[1] This topology leads to useful properties such as multivalency at the surface and shielding effects at the core, which can be exploited for various industrial and biomedical applications, including catalysis,[2] drug delivery,[3] and molecular recognition.[4]

Determining the three-dimensional structure of dendrimers is a major challenge. Recently Müllen and co-workers have succeeded in the tour de force of obtaining the first single-crystal X-ray structure of a polyaryl dendrimer, a special type of

* To whom correspondence should be addressed. Fax: + 41 31 631 80 57.

(1) (a) Newkome, G. R.; Moorefield, C. N.; Vögtle, F. *Dendritic Molecules: Concepts, Synthesis, Applications*; VCH: Weinheim, Germany, 2001. (b) Tomalia, D. A.; Dvornic, P. R. *Nature (London)* **1994**, *372*, 617–618. (c) Smith, D. K.; Diederich, F. *Top. Curr. Chem.* **2000**, *210*, 183–227. (d) Helms, B.; Fréchet, J. M. J. *Adv. Synth. Catal.* **2006**, *348*, 1125–1148. (e) Smith, D. K.; Diederich, F. *Chem.−Eur. J.* **1998**, *4*, 1353–1361. (f) Liang, C.; Fréchet, J. M. J. *Prog. Polym. Sci.* **2005**, *30*, 385–402. (g) Grayson, S. M.; Fréchet, J. M. J. *Chem. Rev.* **2001**, *101*, 3819–3868. (h) Lee, C. C.; Mackay, J. A.; Fréchet, J. M. J.; Szoka, F. C. *Nat. Biotechnol.* **2005**, *23*, 1517–1526.

(2) For reviews of catalytic dendrimers, see: (a) Helms, B.; Fréchet, J. M. J. *Adv. Synth. Catal.* **2006**, *348*, 1125–1148. (b) Kofoed, J.; Reymond, J.-L. *Curr. Opin. Chem. Biol.* **2005**, *9*, 656–664. (c) D. Méry, D.; Astruc, D. *Coord. Chem. Rev.* **2006**, *250*, 1965–1979. (d) Oosterom, G. E.; Reek, J. N. H.; Kamer, P. C. J.; Van Leeuwen, P. W. N. M. *Angew. Chem., Int. Ed.* **2001**, *40*, 1828–1849. (e) Twyman, L. J.; King, A. S. H.; Martin, I. K. *Chem. Soc. Rev.* **2002**, *31*, 69–82.

(3) (a) Liu, M.; Fréchet, J. M. J. *PSTT* **1999**, *2*, 393–401. (b) Yiyun, C.; Tongwen, X. *Eur. J. Med. Chem.* **2005**, *40*, 1188–1192. (c) Morgan, M. T.; Carnahan, M. A.; Immoos, C. E.; Ribiero, A. A.; Finkelstein, S.; Lee, S. J.; Grinstaff, M. W. *J. Am. Chem. Soc.* **2003**, *125*, 15485–15489.

10.1021/jo802743c CCC: $40.75 © 2009 American Chemical Society
Published on Web 04/17/2009

particularly conformationally rigid dendrimer.[5] Most dendrimers, such as those derived from polypropylene imine (PPI), poly(amidoamine) (PAMAM), or Frechet's type dendrimers, are, however, conformationally quite flexible and have so far escaped a full structure determination. Nevertheless, insights into their internal structure have been obtained by various spectroscopic and viscosimetry studies, illuminating the possible backfolding of the flexible branches,[6] the detailed distribution profile of the monomers inside the dendrimer,[7] the structural response to the change of the polarity of the medium,[8] and the properties of the internal hydrogen bonding.[9]

The necessity to interpret experimental data by using detailed atomic models of the dendrimers as opposed to statistical models was pointed out early on.[9] Indeed, molecular dynamics simulations have been performed on various dendrimer types to understand their structural properties,[10] in particular with poly(amidoamine) (PAMAM) dendrimers.[11] These investigations confirm the conformational flexibility of dendrimers and suggest substantial backfolding of external branches inducing a high density located between the core and the periphery leaving some of the inner parts of the dendrimer accessible. This model is supported experimentally by SANS and SAXS studies.[12]

Recently, we reported the preparation of peptide dendrimers[13] formed by alternating proteinogenic amino acids with branching diamino acids (e.g., L-2,3-diaminopropionic acid (Dap) or lysine) during peptide synthesis.[14] We have identified peptide dendrimers with a variety of functions such as catalysis,[15] protein and cofactor binding,[16] and drug delivery.[17] Like most dendrimers, these peptide dendrimers consist of conformationally flexible dendrons and so far have not yielded to direct structural determination by crystallography or NMR. Herein we report the first molecular dynamics study of such peptide dendrimers as the example of a series of peptide dendrimer enzyme models with a catalytic site at their core. The molecular dynamics simulations are combined with substrate docking to provide a detailed picture of the dendrimer structure and an understanding of their experimental structural and kinetic properties. The present investigations provide an unprecedented insight into the molecular dynamics of peptide dendrimers, which might be of general relevance in the context of other conformationally flexible dendrimers.

Results and Discussion

We recently reported a series of third generation dendrimer enzyme models **RG3/RMG3** and **HG3/HMG3** catalyzing the hydrolysis of hydroxypyrene trisulfonate acetate ester **1a** and butyrate ester **1b** in aqueous buffer with substrate binding and multiple turnover (Scheme 1).[18] These dendrimers possess a single catalytic site consisting of a pair of protonated arginine or histidine residues in the first generation branch for substrate binding and a histidine residue at the core performing the catalytic ester hydrolysis reaction. This catalytic core is surrounded by layers of aromatic or hydrophobic residues formed by the second and third generation branches of the dendrimer. Structure−activity relationship studies showed that a positive dendritic effect on the specificity constant k_{cat}/K_M occurs in the arginine-containing "**R**" series dendrimers **RG1→RG3** and **RMG1→RMG3** upon addition of the outer layers of aromatic residues, which is largely mediated by an increase in substrate binding ($1/K_M$) while the catalytic rate constant k_{cat} is preserved. By contrast there is no strong increase of either catalytic proficiency or substrate binding in the "**H**" series dendrimers **HG1→HG3** and **HMG1→HMG3** with three histidine residues at the core and hydrophobic residues in the outer layers (Figure 1).

Structural investigations by NMR show a predominance of sharp signals for the individual amino acid side chains and no cross-peaks in ROESY experiments, suggesting rapid conformational equilibria. Furthermore, CD spectra are typical for random coils. Analysis of the hydrodynamic radii by diffusion NMR gives compaction factors[19] typical for a molten globule state of proteins, indicative of partial folding. The "**R**" series dendrimers are slightly more compact than the "**H**" series dendrimers, yet this difference might not be sufficient to explain the different dependence of catalytic parameters as a function of generation number between the two series. We therefore set out to model their structure by molecular dynamics simulations to gain a closer insight into the structure−activity relationship of catalysis.

(4) (a) Zeng, F.; Zimmerman, S. C. *Chem. Rev.* **1997**, *97*, 1681–1712. (b) Hecht, S.; Fréchet, J. M. J. *Angew. Chem., Int. Ed.* **2001**, *40*, 74–91. (c) Jansen, J. F. G. A.; de Brabander-van den Berg, E. M. M.; Meijer, E. W. *Science* **1994**, *266*, 1226–1229.

(5) Bauer, R. E.; Enkelmann, V.; Wiesler, U. M.; Berresheim, A. J.; Müllen, K. *Chem.—Eur. J.* **2002**, *8*, 3858–3864.

(6) (a) Lescanec, R. L.; Muthukumar, M. *Macromolecules* **1990**, *23*, 2280–2288. (b) Mourey, T. H.; Turner, S. R.; Rubinstein, M.; Fréchet, J. M. J.; Hawker, C. J.; Wooley, K. L. *Macromolecules* **1992**, *25*, 2401–2406. (c) Welch, P.; Muthukumar, M. *Macromolecules* **1998**, *31*, 5892–5897. (d) Gorman, C. B.; Hager, M. W.; Parkhurst, B. L.; Smith, J. C. *Macromolecules* **1998**, *31*, 815–828. (e) Boris, D.; Rubinstein, M. *Macromolecules* **1996**, *29*, 7251–7260.

(7) Rosenfeldt, S.; Dingenouts, N.; Ballauff, M.; Werner, N.; Vögtle, F.; Lindner, P. *Macromolecules* **2002**, *35*, 8098–8105.

(8) (a) De Backer, S.; Prinzie, Y.; Veheijen, W.; Smet, M.; Desmedt, K.; Dehaen, W.; De Schryver, F. C. *J. Phys. Chem. A* **1998**, *102*, 5451–5455. (b) Chai, M.; Niu, Y.; Youngs, W. J.; Rinaldi, P. L. *J. Am. Chem. Soc.* **2001**, *123*, 4670–4678. (c) Chen, W.; Tomalia, D. A.; Thomas, J. L. *Macromolecules* **2000**, *33*, 9169–9172.

(9) Bosman, A. W.; Bruining, M. J.; Kooijman, H.; Spek, A. L.; Janssen, R. A. J.; Meijer, E. W. *J. Am. Chem. Soc.* **1998**, *120*, 8547–8548.

(10) (a) Ballauff, M.; Likos, C. N. *Angew. Chem., Int. Ed.* **2004**, *43*, 2998–3020. (b) Suek, N. W.; Lamm, M. H. *Macromolecules* **2006**, *39*, 4247–4255. (c) Lescanec, R. L.; Muthukumar, M. *Macromolecules* **1990**, *23*, 2280–2288.

(11) (a) Lin, S.-T.; Maiti, P. K.; Goddard, W. A., III. *J. Phys. Chem. B* **2005**, *109*, 8663–8672. (b) Maiti, P. K.; Çağin, T.; Lin, S.-T.; Goddard, W. A. *Macromolecules* **2005**, *38*, 979–991. (c) Mansfield, M. L.; Klushin, L. I. *Macromolecules* **1993**, *26*, 4262–4268.

(12) (a) Rathgeber, S.; Pakula, T.; Urban, V. *J. Chem. Phys.* **2004**, *121*, 3840–3853. (b) Pötschke, D.; Ballauff, M.; Lindner, P.; Fischer, M.; Vögtle, F. *Macromol. Chem. Phys.* **2000**, *201*, 330–339.

(13) (a) Crespo, L.; Sanclimens, G.; Pons, M.; Giralt, E.; Royo, M.; Albericio, F. *Chem. Rev.* **2005**, 1663–1681. (b) Sadler, K.; Tam, J. P. *Rev. Mol. Biotechnol.* **2002**, *90*, 195–229. (c) Darbre, T.; Reymond, J.-L. *Acc. Chem. Res.* **2006**, *39*, 925–934.

(14) (a) Esposito, A.; Delort, E.; Lagnoux, D.; Djojo, F.; Reymond, J.-L. *Angew. Chem., Int. Ed.* **2003**, *42*, 1381–1383. (b) Lagnoux, D.; Delort, E.; Douat-Casassus, C.; Esposito, A.; Reymond, J. L. *Chem.—Eur. J.* **2004**, *10*, 1215–1226. (c) Douat-Casassus, C.; Darbre, T.; Reymond, J.-L. *J. Am. Chem. Soc.* **2004**, *126*, 7817–7826. (d) Clouet, A.; Darbre, T.; Reymond, J.-L. *Adv. Synth. Catal.* **2004**, *346*, 1195–1204.

(15) (a) Kofoed, J.; Darbre, T.; Reymond, J.-L. *Org. Biomol. Chem.* **2006**, 3268–3281. (b) Delort, E.; Nguyen-Trung, N.-Q.; Darbre, T.; Reymond, J.-L. *J. Org. Chem.* **2006**, *71*, 4468–4480. (c) Delort, E.; Darbre, T.; Reymond, J.-L. *J. Am. Chem. Soc.* **2004**, *126*, 15642–15643.

(16) (a) Kolomiets, E.; Johansson, E. M. V.; Renaudet, O.; Darbre, T.; Reymond, J.-L. *Org. Lett.* **2007**, *9*, 1465–1468. (b) Sommer, P.; Uhlich, N.; Reymond, J.-L.; Darbre, T. *ChemBioChem* **2008**, *9*, 689–693.

(17) Lagnoux, D.; Darbre, T.; Schmitz, M. L.; Reymond, J.-L. *Chem.—Eur. J.* **2005**, *11*, 3941–3950.

(18) Javor, S.; Delort, E.; Darbre, T.; Reymond, J.-L. *J. Am. Chem. Soc.* **2007**, *129*, 13238–13246.

(19) Wilkins, D. K.; Grimshaw, S. B.; Receveur, V.; Dobson, C. M.; Jones, J. A.; Smith, L. J. *Biochemistry* **1999**, *38*, 16424–16431.

(20) (a) van der Spoel, D.; Lindahl, E.; Hess, B.; Groenhof, G.; Mark, A. E.; Berendsen, H. J. C. *J. Comput. Chem.* **2005**, *26*, 1701–1718. (b) Lindahl, E.; Hess, B.; van der Spoel, D. *J. Mol. Model.* **2001**, *7*, 306–317.

SCHEME 1. Dendrimer-Catalyzed Ester Hydrolysis and Dendrimer Structures[a]

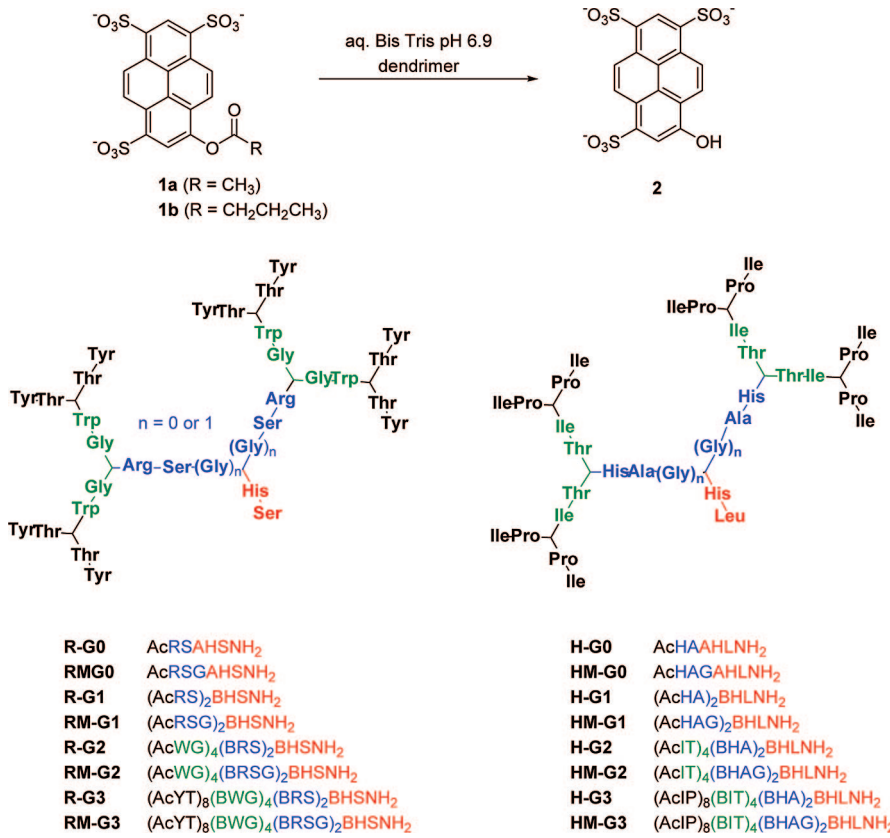

R-G0	$AcRSAHSNH_2$	**H-G0**	$AcHAAHLNH_2$
RMG0	$AcRSGAHSNH_2$	**HM-G0**	$AcHAGAHLNH_2$
R-G1	$(AcRS)_2BHSNH_2$	**H-G1**	$(AcHA)_2BHLNH_2$
RM-G1	$(AcRSG)_2BHSNH_2$	**HM-G1**	$(AcHAG)_2BHLNH_2$
R-G2	$(AcWG)_4(BRS)_2BHSNH_2$	**H-G2**	$(AcIT)_4(BHA)_2BHLNH_2$
RM-G2	$(AcWG)_4(BRSG)_2BHSNH_2$	**HM-G2**	$(AcIT)_4(BHAG)_2BHLNH_2$
R-G3	$(AcYT)_8(BWG)_4(BRS)_2BHSNH_2$	**H-G3**	$(AcIP)_8(BIT)_4(BHA)_2BHLNH_2$
RM-G3	$(AcYT)_8(BWG)_4(BRSG)_2BHSNH_2$	**HM-G3**	$(AcIP)_8(BIT)_4(BHAG)_2BHLNH_2$

[a] The C-terminus of the peptide chains are at the core as carboxamide, the branching points are L-2,3-diaminopropionic acid (B in the linear formula) and the *N*-termini are acetylated (Ac). Codes for amino acids: Tyr = Y = L-tyrosine, Thr = T = L-threonine, Trp = W = L-tryptophane, Gly = G = glycine, Arg = R = L-arginine, Ser = S = L-serine, His = H = L-histidine, Ile = I = L-isoleucine, Pro = P = L-proline, Ala = A = L-alanine, Leu = L = L-leucine.

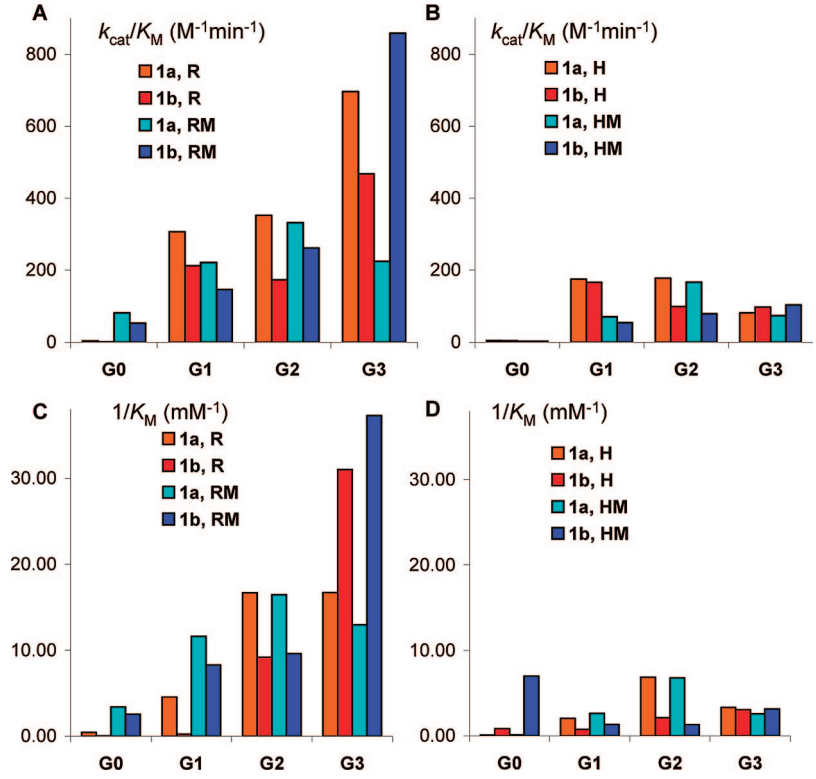

FIGURE 1. Catalytic proficiencies (k_{cat}/K_M, **A**: "R"-dendrimers, **B**: "H"-dendrimers) and substrate binding ($1/K_M$, **C**: "R"-dendrimers, **D**: "H"-dendrimers) of peptide dendrimers as a function of generation number, for the hydrolysis of substrate **1a/b**. Conditions: 3.3, 5.0, or 10 μM dendrimer, 30−1000 μM substrate 10 mM aq. Bis-Tris buffer pH 6.9, 34 °C. Data from ref 18.

Molecular Dynamics. Molecular dynamics were performed with GROMACS,[20] which has been extensively tested in the context of protein modeling and employs fine-tuned force-field parameters for amino acids relevant to protein structures. Because the program only accepts linear peptides as input, we wrote a topology manipulation kit (TMK) to enable reading of dendritic topologies (see the Supporting Information). Force-field parameters for the Dap branching unit were constructed manually by adapting the CYS residue in the parameter file.

The starting structures of the peptide dendrimers were generated with CORINA,[21] which provided elongated random coil structures avoiding thus any biases toward any folded conformation. To ensure that the trajectory does not depend on the CORINA-generated conformation, each dendrimer was first heated at 800 K for 250 ps, during which the dendrimer size decreased slightly before stabilizing, suggesting a partial packing (Figure S5, Supporting Information). Twenty high-temperature conformations were then sampled every 50 ps, and each conformation was progressively cooled to 300 K during 4 ns. The cooling led to an additional collapse of the structure where some of the apolar residues were kept inside the globule and were thus shielded from the solvent, an effect reminiscent of the hydrophobic collapse during protein folding (Figure 2). The resulting set of 20 low-energy conformations was used as a representation of the available conformational space for each dendrimer. This procedure, which is similar to folding simulations as reported for example for the Trp-cage protein,[22] was selected as the most appropriate to generate a model structure in the absence of an experimental structure.

Model Validation. The hydrodynamic radius of the models was estimated and compared with the data from the diffusion NMR.[23] Several theoretical methods have been developed to predict the hydrodynamic properties of molecules from their atomic coordinates.[24] Methods emphasizing modeling of the outer shell[25] are the most suited to describe the hydrodynamic behavior of macromolecules.[26] However, they are based on complex algorithms and are computationally expensive. For spherical molecules, the Stokes radius is an approximation of the hydrodynamic radius. The analysis of the overall dendrimer shape in our models has shown that the dendrimers are indeed close to a sphere (data not shown). The hydrodynamic radius of the solvated dendrimer model was therefore obtained by fitting the radial distribution function of the solvent molecules around the center of mass of the dendrimer. The hydrodynamic radius was taken at the end of the steep portion of the water distribution function (i.e., distance at 0.95 of the density of the bulk water, Figure S6 in the Supporting Information). The values obtained by this method were in excellent agreement with the values from the diffusion-NMR experiments (Table 1, Figure 3), especially for the higher generation dendrimers, confirming the hydrophobic collapse of the structure as suggested by MD (the same analysis on the extended conformations produced by CORINA gave significantly higher radii in all cases).

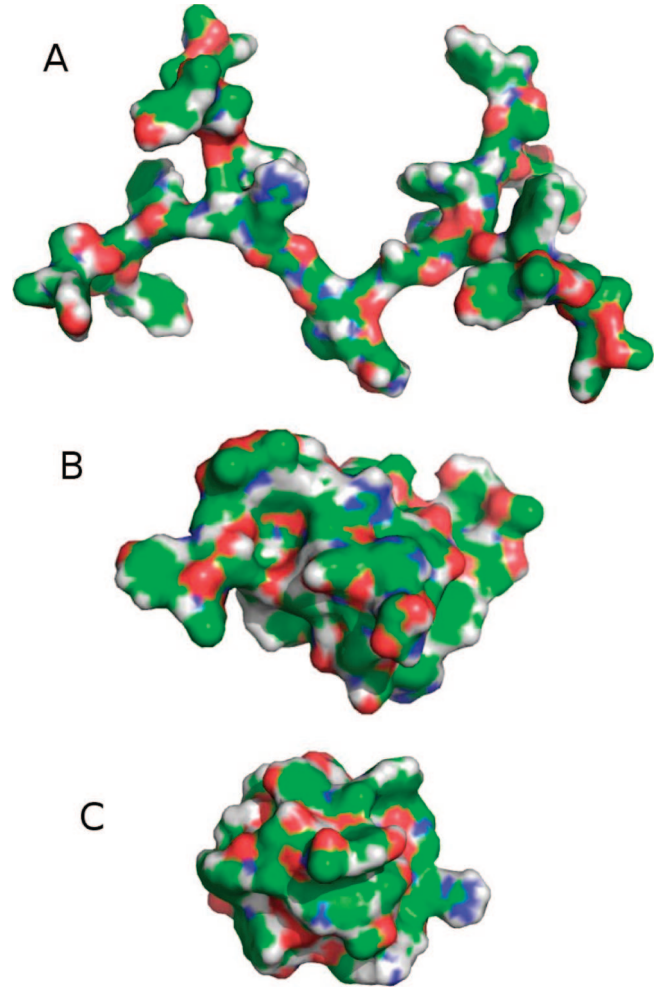

FIGURE 2. Surface representation of the **RMG3** dendrimer in the course of the simulated annealing. The carbons are in green, nitrogens in blue, oxygens in red, hydrogens in white. (A) CORINA structure; (B) conformation at 800 K; (C) conformation at 300 K. The 800 K structure was sampled after 1050 ps, and the 300 K conformation is obtained after cooling this structure.

TABLE 1. Hydrodynamic Radii Determined by PGSE-NMR and MD[a]

dendrimer	exptl r_H (nm)	calcd r_H (nm)
HG1	0.81	0.91
HG2	1.13	1.17
HG3	1.56	1.44
HMG1	0.86	0.92
HMG2	1.22	1.20
HMG3	1.62	1.51
RG1	0.79	0.88
RG2	1.04	1.18
RG3	1.44	1.46
RMG1	0.86	0.94
RMG2	1.11	1.17
RMG3	1.52	1.52

[a] For comparison the rdf in the CORINA G3 dendrimers models were 13−35% above the experimental values. The accuracy of PGSE-NMR using a probe head generating 50×10^{-4} T·cm^{-1} gradients is estimated at ±5%.

Analysis of Inter-residue Contacts. In native proteins folding induces close contacts between residues remote in the sequence. To probe if a related folding occurred in the peptide dendrimers, through-space shortest distances between all residue

(21) Sadowski, J.; Gasteiger, J.; Klebe, G. *J. Chem. Inf. Comput. Sci.* **1994**, *34*, 1000–1008.
(22) (a) Zhou, R. *Proc. Natl. Acad. Sci. U.S.A.* **2003**, *100*, 13280–13285. (b) Juraszek, J.; Bolhuis, P. G. *Proc. Natl. Acad. Sci. U.S.A.* **2006**, *103*, 15859–15864. (c) Juraszek, J.; Bolhuis, P. G. *Biophys. J.* **2008**, *95*, 4246–4257.
(23) Cohen, Y.; Avram, L.; Frish, L. *Angew. Chem., Int. Ed.* **2005**, *44*, 520–554.
(24) Garcia de la Torre, J.; Huertas, M. L.; Carrasco, B. *Biophys. J.* **2000**, *78*, 719–730.
(25) (a) Filson, D. P.; Bloomfield, V. A. *Biochemistry* **1967**, *6*, 1650–1658. (b) Bloomfield, V. A.; Filson, D. P. *J. Polym. Sci. Part C* **1968**, *25*, 73–83.
(26) Carrasco, B.; Garcia de la Torre, J. *Biophys. J.* **1999**, *76*, 3044–3057.

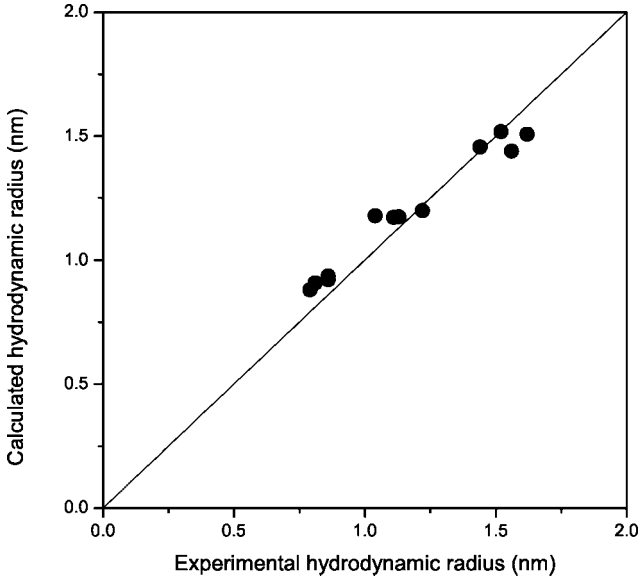

FIGURE 3. Correlation between hydrodynamic radii as experimentally determined (*x*-axis) and as estimated by MD (*y*-axis). Data from Table 1.

pairs in the dendrimers were determined and plotted as a function of their topological distance (the number of residues in the shortest connecting path) in the structure (Figure 4). Indeed close contacts between remote residues were found in the low-energy conformers up to the longest possible topological distances, representing contacts between different branches of the dendrimers (Figure 4A). However, the minimal distance between residues at topological distances above 10 residues raised above 10 nm when averaged over the 20 low-energy conformers of each dendrimer, highlighting the diversity of the 20 energy-minimized conformers (Figure 4B). Nevertheless, these averaged through-space inter-residue distances were still much shorter than those averaged at high temperature (Figure 4C) or for the extended CORINA structure (Figure 4D), reflecting the molten globule state of the dendrimer in its low-energy conformations at 300 K. The fact that the averaged through-space distance in the low-energy conformers (Figure 4B) is independent of the topological distance above 10 residues suggests that residues in the second and third generation layer have a similar potential to modify the environment of the active core and influence catalysis.

Intramolecular Hydrogen Bonds in Peptide Dendrimers. Intramolecular hydrogen bonds leading to secondary structures are essential stabilizing elements in folded proteins. To determine if an H-bond exists, the GROMACS default geometrical criterion was used, $d \leq 0.35$ nm and $\alpha < 30°$,[27] which is a cutoff value that should be sufficient to detect any significant H-bonds[28] involving backbone amides[29] and/or side chain functional groups. The analysis showed that most intramolecular H-bonds in the dendrimers were backbone-to-backbone H-bonds. Interestingly, the number of backbone-to-backbone H-bonds per residue increased with the generation number in all four series. However, their number remained too low for secondary structure elements to be formed (≤0.33 H-bond per residue in the dendrimers vs. 1 in α-helices or β-sheets) (Table 2). The low ratio of backbone-to-backone hydrogen bond per residue might explain the high conformational flexibility of the dendrimers. Conformational flexibility is also illustrated by the fact that most H-bonds were observed only once across the 20 low-energy conformers. On the other hand, approximately half of the backbone-to-backbone hydrogen bonds (which make up 88% of the total H-bonds observed in G3 dendrimers) occurred between residues $i \leftrightarrow i + 2$, $i \leftrightarrow i + 3$, and $i \leftrightarrow i + 4$, which are relative positions found in β-turns and α-helices, highlighting that some of the H-bonding structure of dendrimers is related to that found in folded proteins (Figure 5). We have recently showed that α-helices can indeed be incorporated into peptide dendrimers.[30]

Docking. As shown previously, the pH−rate profile and structure−activity relationships of catalysis suggest that substrate binding by the dendrimers occurs primarily by electrostatic interactions between the pair of protonated arginine ("R"-series) or histidine ("H"-series) residues in the first generation branch, while the core histidine residue acts as a general base or nucleophile. Due to their polarity, the cationic and nucleophilic groups were indeed found at the dendrimer surface in all conformers analyzed. These residues were placed in positions compatible with binding and catalysis. Their relative distance (1.0−1.2 nm) was very close to the two longer of the three ester-to-sulfonate distances in the substrates (0.54, 1.0, and 1.2 nm). This distance increased by 0.2−0.3 nm between the **G1** and the **G3** dendrimer in all four series; however, the distances varied strongly between individual conformers, precluding a simple interpretation of catalysis in terms of geometrical distances between reactive groups (Figure S7, Supporting Information). A docking study was therefore undertaken to see if the dendrimer models were compatible with binding of substrate **1** and catalysis. Docking usually accurately predicts the binding mode of ligands to proteins,[31] and provides an estimate of the binding energy. This method should be suitable to gain an insight into the substrate−dendrimer interactions.[32] It should be noted that the substrate−dendrimer interactions could not be measured directly due to precipitation of the dendrimers in the presence of substrate in attempted NMR and ITC measurements.

For each dendrimer, substrate **1b** was docked 10 times onto each of the 20 low-energy conformations obtained from the MD simulation. In all docking runs the estimated docking energy of the substrate was lower than −3 kcal/mol. The best docking run in each of the 20 low-energy conformations was used to calculate an average docked energy for each substrate−dendrimer pair. The average values were comprised between −5 and −6 kcal/mol, which is indistinguishable within the interpretable range of estimated docking energies. Binding was generally mediated by 2 to 3 hydrogen bonds and 5 to 6 van der Waals contacts (Table 3). For each dendrimer 60−80% of the docking runs resulted in at least one salt-bridge formed between a sulfonate and a cationic residue. In some cases, a bidentate binding mode was observed where both of the cations bind two

(27) See the GROMACS user manual. http://www.gromacs.org 10/2008.

(28) O−H···O (long) = 0.28 nm; OH···N = 0.26−0.30 nm; NH···O = 0.26−0.33 nm; NH···N = 0.28−0.32 nm; OH···O (ice) = 0.27−0.28 nm. Angle: ideally 0°. Angle >40° "bonding must become minimal", as cited from the following: Speakman, J. C. *The hydrogen bond and other intermolecular forces*; The Chemical Society: London, UK, 1975.

(29) (a) Karle, I. L.; Balaram, P. *Biochemistry* **1990**, *29*, 6747–6756. (b) Cotesta, S.; Stahl, M. *J. Mol. Model.* **2006**, *12*, 436–444.

(30) Javor, S.; A.; Natalello, A.; Doglia, S. M.; Reymond, J.-L. *J. Am. Chem. Soc.* **2008**, *130*, 17248–17249.

(31) Park, H.; Lee, J.; Lee, S. *Proteins* **2006**, *65*, 549–554.

(32) A direct molecular dynamics simulation of substrate−dendrimer interactions would require extensive simulation (>50 ns per conformer) to produce interpretable data, and was not accessible within the available computing time.

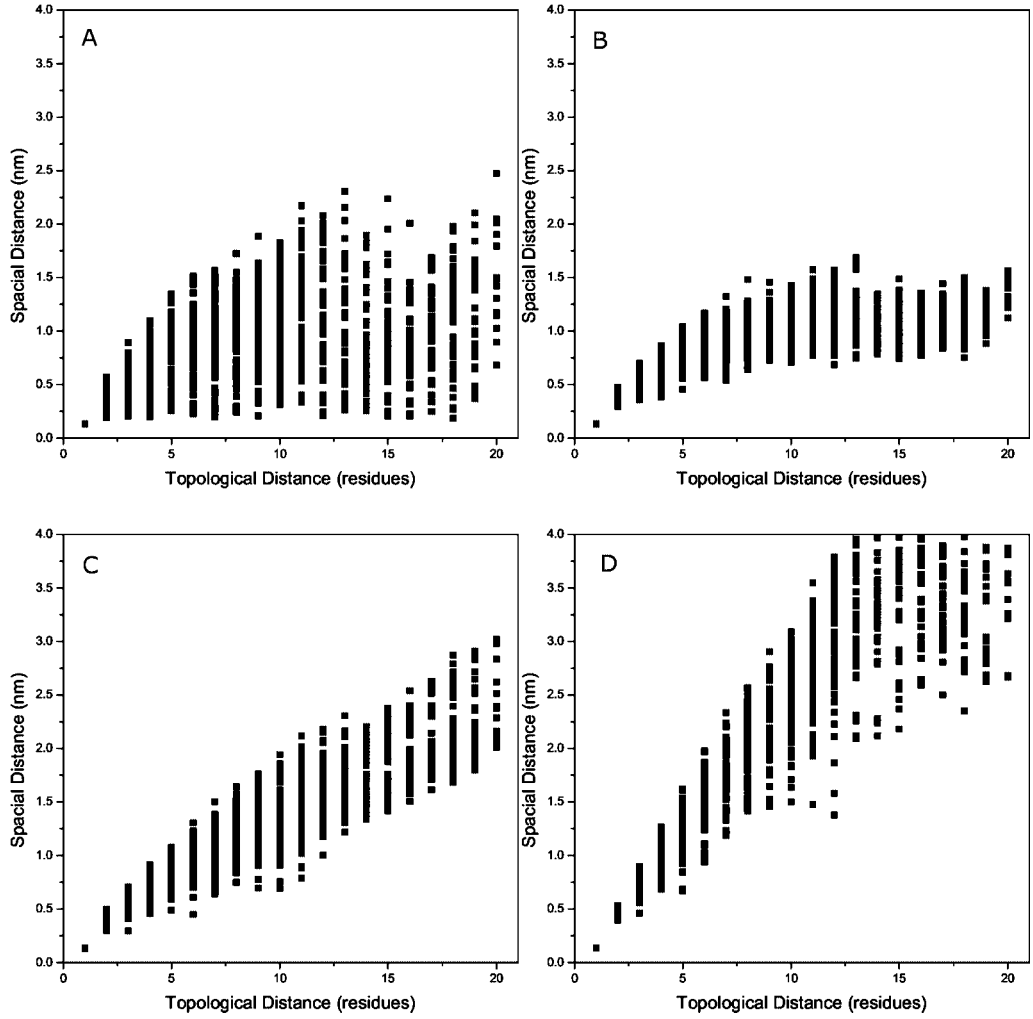

FIGURE 4. Through-space distance as a function of the topological distance: (A) a low energy conformer of **RMG3**; (B) **RMG3** average over 20 energy-minimized conformers at 300 K; (C) Average over 20 conformers at 800 K; and (D) CORINA. Similar plots are obtained for the analysis of **RG3**, **HMG3**, and **HG3** (data not shown).

TABLE 2. Hydrogen Bond Counts Summed over the 20 Low-Energy Conformations of Each Peptide Dendrimer

		all H-bonds[a]		backbone H-bonds[b]		conserved H-bonds in *n* conformers[c]			
dendrimer	AA[d]	total	HB/conf	total	HB/res./conf[e]	$n \geq 4$	$n = 3$	$n = 2$	$n = 1$
HG1	7	18	0.9	15	0.11		1	1	13
HG2	17	110	5.5	87	0.26	1[f]	2	12	62
HG3	37	241	12.1	212	0.29	1	8	14	188
HMG1	8	32	1.6	31	0.19		1	5	21
HMG2	18	131	7.0	120	0.33	1[g]	4	17	88
HMG3	38	249	12.5	216	0.28	3	8	17	179
RG1	7	33	1.7	15	0.11			3	27
RG2	17	105	5.3	76	0.22		4	7	87
RG3	37	370	18.5	239	0.32	2	3	25	303
RMG1	8	43	2.2	25	0.16		1	7	26
RMG2	18	149	7.5	113	0.31	1	1	14	114
RMG3	38	372	18.7	241	0.32	3	2	19	316

[a] The cutoff distance is 0.35 nm and the maximum bond angle is 30°. [b] Only backbone-to-backbone H-bonds. [c] Count of H-bonds that appear in *n* different conformers. [d] Total number of amino acids in the dendrimer, including branching diamino acids. [e] Number of backbone-to-backbone H-bonds per residue per conformer. [f] Found in 6 conformers. [g] Found in 5 conformers.

different sulfonates in the same complex. Similar binding modes were experimentally evidenced for other cationic dendrimers binding an anionic substrate.[33]

To test if the docked poses were also compatible with the esterolysis mechanism, the distance between the nucleophilic histidine residue and the labile ester carbonyl group was analyzed. In most conformations, the average distances were much too long for a direct reaction to take place. Nevertheless,

(33) (a) Banerjee, D.; Broeren, M. A. C.; van Genderen, M. H. P.; Meijer, E. W.; Rinaldi, P. L. *Macromolecules* **2004**, *37*, 8313–8318. (b) Broeren, M. A. C.; de Waal, B. F. M.; van Genderen, M. H. P.; Sanders, H M. H. F.; Fytas, G.; Meijer, E. W. *J. Am. Chem. Soc.* **2005**, *127*, 10334–10343.

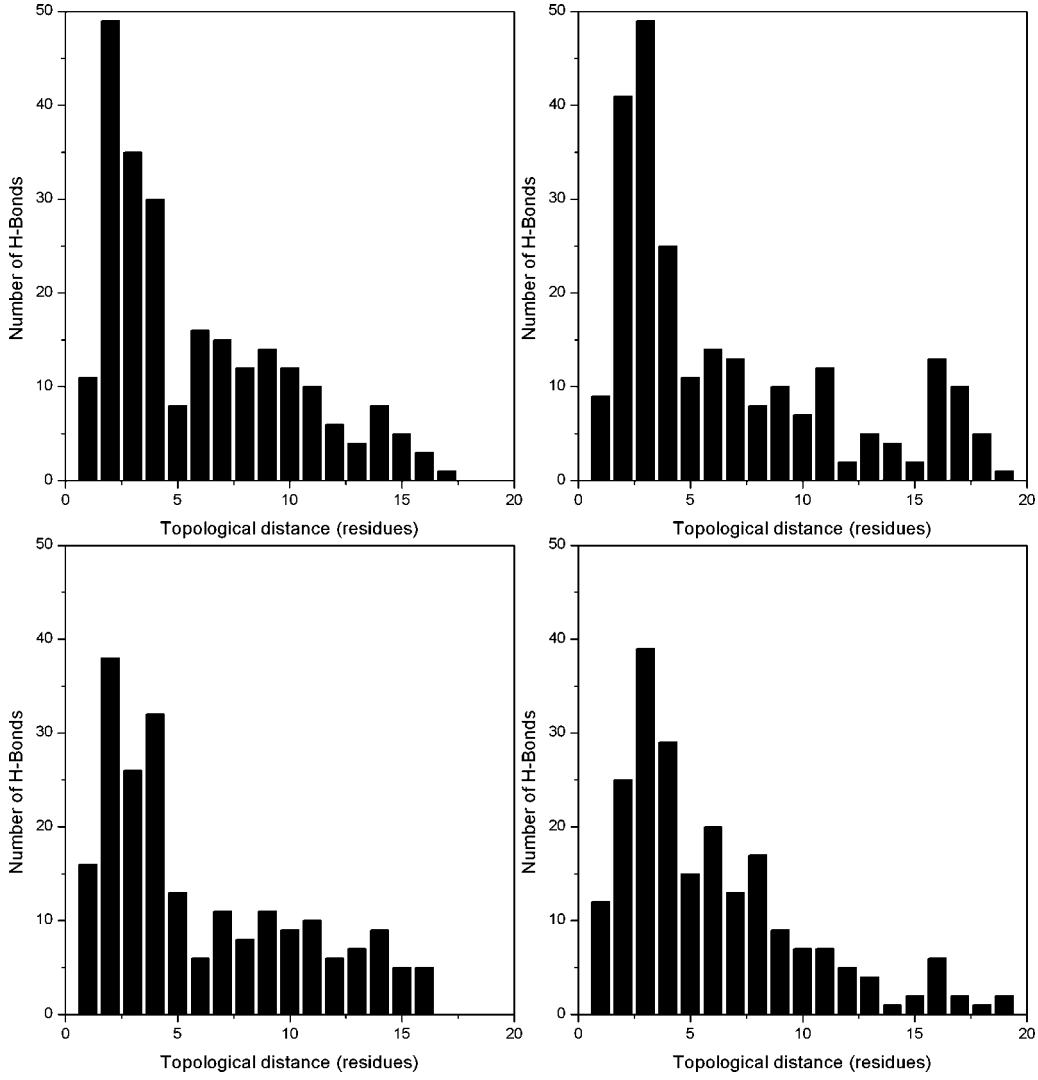

FIGURE 5. Inter-residue distance of backbone hydrogen bonds in **RG3** (top left), **RMG3** (top right), **HG3** (bottom left), and **HMG3** (bottom right) at 300 K in water. The total number of backbone-to-backbone H-bonds over the 20 low-energy conformers is shown as a function of inter-residue distance.

TABLE 3. Docked Energies and Contacts in the Substrate 1b Esterase Dendrimer Complexes

	docked energy (kcal/mol)[a]		Contact with pair of protonated Arg or His at G1[b]				Other contacts with the dendrimer[b]			
dendrimer	avg	±σ	H-bonds	±σ	van der Waals	±σ	H-bonds	±σ	van der Waals	±σ
HG1	−5.22	0.61	0.80	0.70	1.38	0.64	1.51	0.79	3.83	1.16
HG2	−5.37	0.74	0.62	0.65	1.12	0.66	1.65	0.87	4.65	1.19
HG3	−5.58	0.61	0.62	0.65	0.93	0.71	1.65	0.85	5.26	1.48
HMG1	−5.00	0.53	0.81	0.68	1.28	0.68	1.56	0.73	4.09	1.07
HMG2	−5.30	0.56	0.39	0.64	0.95	0.60	1.59	0.93	4.75	1.38
HMG3	−5.42	0.72	0.64	0.61	0.96	0.68	1.51	0.89	5.18	1.30
RG1	−5.60	0.76	1.15	0.73	1.18	0.62	2.01	0.73	3.48	1.07
RG2	−5.79	0.72	0.87	0.71	0.80	0.71	1.90	0.92	4.26	1.48
RG3	−5.50	0.44	0.65	0.61	0.69	0.80	1.94	1.02	4.91	1.42
RMG1	−5.59	0.93	1.23	0.70	1.08	0.74	2.11	0.83	3.64	1.00
RMG2	−5.86	0.68	1.11	0.75	0.90	0.69	1.97	0.79	4.12	1.28
RMG3	−5.67	0.74	0.88	0.79	0.83	0.79	2.08	0.90	4.63	1.30

[a] For each dendrimer, the docking energy is the average of the best docking energy from 10 docking runs for each of the 20 low-energy conformers. [b] All contacts were calculated with Ligplot.[34] Values are averaged over the computed 200 low-energy poses.

at least one of the docking poses in one of the low-energy conformers of each dendrimer showed a short enough distance to allow either a general base catalyzed reaction mechanism with intervening water molecule (<5.0 Å) or a direct nucleophilic attack of the ester carbonyl by the nucleophilic histidine side chain (<3.5 Å). Most of these potentially reactive conformations showed only a single binding salt-bridge between substrate and dendrimer, reflecting a two-point binding rather that a three-point binding mode of the substrate, although the tighter three-point binding mode was also observed.

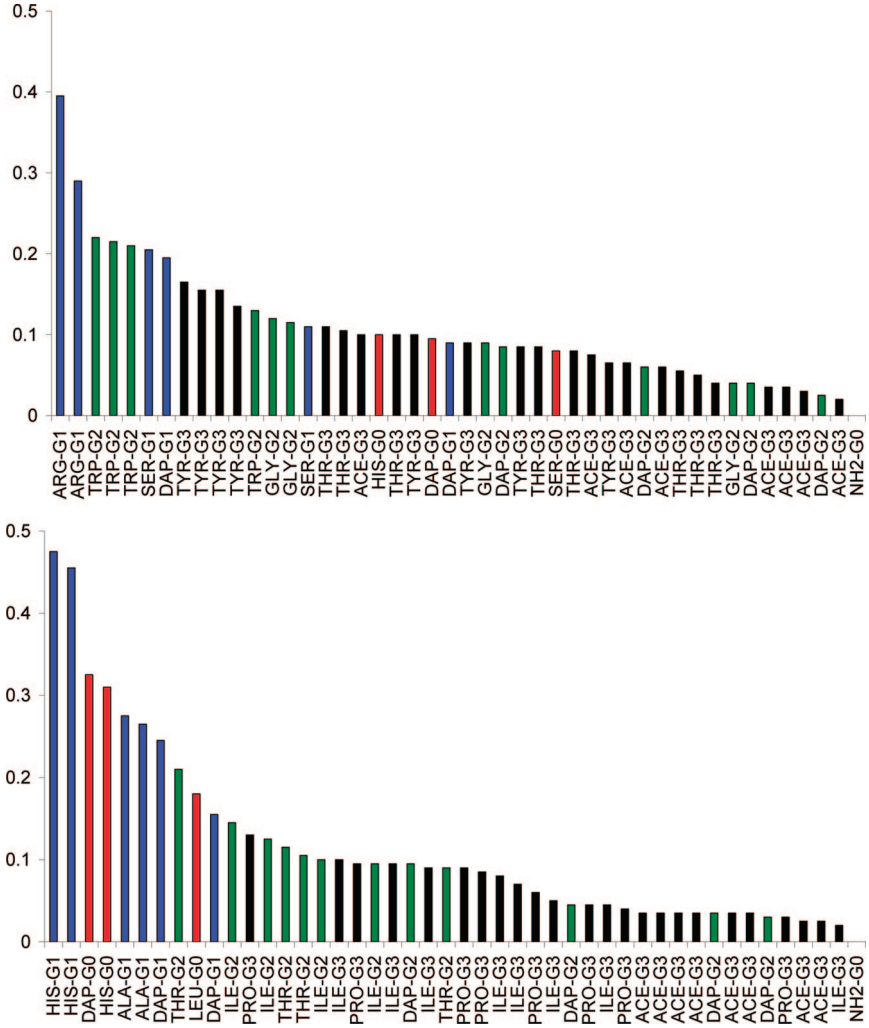

FIGURE 6. van der Waals contacts between substrate **1** and dendrimers **RG3** (upper) and **HG3** (lower) as estimated by docking. The average number of van der Waals contacts to each residue across 200 docked complexes (20 dendrimer conformers × 10 docking runs) is plotted as a function of residue number. Residues are ordered in descending order of contact frequency. Bars are color coded by the generation number (red = G0, blue = G1, green = G2, black = G3, see also Scheme 1 and Figure 7).

While both the "R" and the "H" series dendrimers produced comparable results in terms of structural models and electrostatic binding mode of the substrate, a remarkable difference was found in the nature of the van der Waals contacts to substrate **1b** predicted by docking. Van der Waal contacts between **1b** and **RG3** mostly involved the tryptophan residues in G2 and tyrosine residues in G3, while the core residues were not involved. By contrast, in **HG3** van der Waals contacts to substrate **1b** concerned mostly residues in the dendrimer core, while the outer layers at generation G2 and G3 were not involved in binding (Figure 6). The propensity of **RG3** to make contacts to **1b** via the outer branches and of **HG3** via the dendrimer core was readily visible in individual docked poses (Figure 7). The same trend was observed in dendrimers **RMG3** and **HMG3**, as well as at the level of the G2 dendrimers. Thus, van der Waals contacts to the tryptophan residues were very frequent in **RG2** and **RMG2**, while contacts with residues in the G0 and G1 branch were most frequent in **HG2** and **HMG2** (Figure S8, Supporting Information).

The aromatic residues in the outer layers of the "R" dendrimers thus allow productive van der Waals contacts during docking of substrate **1b**. Such contacts do not take place with the hydrophobic residues in outer amino acid layers in the "H" dendrimers. This docking trend is consistent with the larger hydrophobic surface of the aromatic residues and their known occurrence in many protein binding sites such as those of antibodies. The difference observed in docking between "R" and "H" dendrimers closely parallels the observed trend in catalytic proficiencies and substrate binding, which only increase in the "R" dendrimers at higher generation numbers, while the "H" dendrimers show comparable behavior across different generation numbers (Figure 1). The structural model therefore suggests that the positive dendritic effect on catalysis in the "R" series dendrimers is triggered by direct binding interactions between the substrate and the outer dendritic layers of the dendrimers. On the other hand, the absence of a similar binding interaction in the "H" series dendrimers might explain the fact that catalysis is relatively unaffected by the addition of the outer dendritic branches in this series.

Overall the docking analysis shows that although the dendrimers adopt multiple conformations in aqueous solution, the pair of arginine residues and the catalytic histidine are positioned at the dendrimer surface in a relative orientation compatible with binding and catalysis. The conformational equilibria in the

(34) Wallace, A. C.; Laskowski, R. A.; Thornton, J. M. *Protein Eng. Des. Sel.* **1995**, *8*, 127–134.

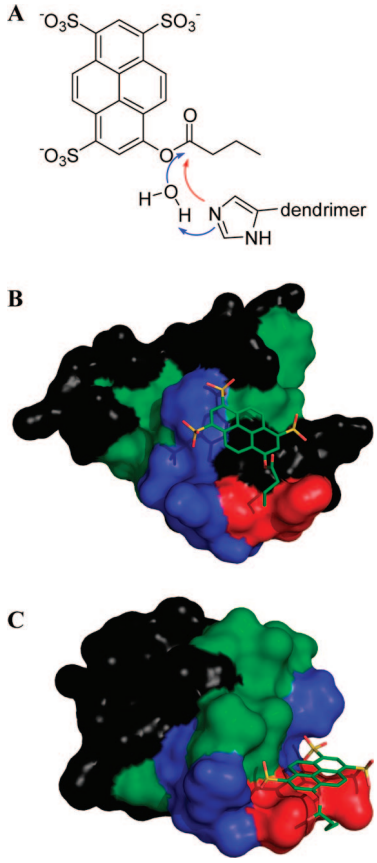

FIGURE 7. Catalysis mechanism and docking. (A) Catalytic role of the core histidine residue as nucleophile (red arrow) or general base (blue arrow). (B) 3-D model of a pose of **RG3** with docked substrate **1b**. (C) 3-D model of a pose of **HG3** with docked substrate **1b**. The dendrimer is shown in surface representation color coded by generation number (red = G0, blue = G1, green = G2, black = G3, see also Scheme 1 and Figure 6). Substrate carbons are represented in green, nitrogens in blue, oxygens in red, and sulfurs in yellow.

dendrimers probably take place much faster than the catalytic turnover, which is relatively slow in these systems. Catalysis therefore probably involves formation of the substrate−dendrimer complex, followed by equilibration between multiple conformations until a catalytically productive orientation is encountered, leading to catalytic turnover.

Methods

Generation of Input Files for Molecular Dynamics. Dendrimer topology files for GROMACS were produced by using in-house software (TMK) described in the Supporting Information. The coordinates of the starting conformations were generated with the commercial software CORINA.

Molecular Dynamics. All the molecular dynamics were carried out with GROMACS 3.2, using the GROMOS-96 43a1 force field[35] under periodic boundary conditions. After generation of the input files (see the Supporting Information), a cubic box was created around the dendrimer at a distance of 0.8 nm from the edge of the molecule and filled with solvent molecules using the simple point charge (SPC) model (density between 969 and 1005 g/L). For each model, the size of the box was kept fixed in the following simulations. The dynamics at pH 2 were performed with all the histidines and arginines protonated. In the models at pH 7 the central (G0) histidine was deprotonated. Electroneutrality was obtained by addition of chloride ions. The system was energy minimized by using the steepest descent algorithm for 500 steps. The equations of motion were integrated by using the leapfrog algorithm with a step size of 2 fs. All bond lengths were constrained to their equilibrium values by using the LINCS algorithm.[36] The neighbor list for the calculation of nonbonded interactions was updated every five timesteps under periodic boundary conditions. A twin range cutoff of 1.0 nm was used for both Coulomb and Lennard-Jones interactions. In all simulations the peptide, the chloride ions, and the solvent were coupled separately to a temperature bath at the desired temperature, using the Berendsen algorithm[37] with a coupling time of 0.1 ps. Initial velocities were obtained from a Maxwellian distribution at the initial temperature of 800 K. A first trajectory was computed at 800 K and high energy conformations were sampled every 50 ps between 250 and 1200 ps. Each of these 20 conformations was used as a staring conformation for a second run 800→600 K in 100 ps then 600→300 K during 3900 ps resulting in 20 low-energy conformations for each dendrimer.

Docking. The docking was performed with the Autodock (v. 3.05) package.[38] The preparation of the receptor and the ligand was done with the MGL Autodock Tools package (ADT). For each dendrimer, the 20 structures after cooling to 300 K were used as receptors. The starting structure of the ligand **1b** was generated by using CORINA and further parametrized with ADT. The allowed conformational space, docking box, was centered on the center of mass of the dendrimer. The grid consisted of 100 × 100 × 100 points with a 0.375 Å spacing. This protocol ensured that the whole dendrimer was considered as a potential binding site. For each dendrimer conformation, 10 runs were performed leading to 200 substrate−dendrimer complexes.

Hydrodynamic Radius of the MD Model. The hydrodynamic radius was determined by fitting the radial distribution of water around the dendrimer. The distance at which the water had a density of 0.95 of the bulk solvent was used as the theoretical hydrodynamic radius.

Experimental Hydrodynamic Radius. The diffusion constant of the dendrimers was obtained by ^{1}H NMR, using a stimulated echo (STE) pulse sequence. The measurements were carried out with dilute solutions (typically 5 mg·mL^{-1}) in D_2O at 300 K. The gradient with a maximum strength of 50 × 10^{-4} T·cm^{-1} was calibrated by using the HOD proton signal in 99.997% D_2O. The diffusion time Δ was 50 ms and the gradient duration δ was 7 ms. The diffusion coefficient D was derived from peak integrals or intensities by using the Simfit software from Bruker. The hydrodynamic radii were calculated from the diffusion coefficient D (Table S1, Supporting Information) by using the Stokes−Einstein equation with η = 1.089 mPa for D_2O at 300 K.

Conclusion

The molecular dynamics and docking study of single-site esterase peptide dendrimers above provide a detailed and consistent model of the conformational and binding properties of peptide dendrimers. The study was facilitated by the availability of the GROMACS force field, which is finely tuned for protein molecular dynamics, is computationally fast, and has an open-source code that could be modified to accept the branched topology of the peptide dendrimers. The suitability of the GROMACS force field to the study of peptide dendrimers was established by the adequation of experimentally determined and predicted hydrodynamic gyration radii across very different sizes (**G1→G3**) for 12 different dendrimers.

(35) Daura, X.; Mark, A. E.; Van Gunsteren, W. F. *J. Comput. Chem.* **1998**, *19*, 535–547.
(36) Hess, B.; Bekker, H.; Berendsen, H. J. C.; Fraaije, J. G. E. M. *J. Comput. Chem.* **1997**, *18*, 1463–1472.
(37) Berendsen, H. J. C.; Postma, J. P. M.; DiNola, A.; Haak, J. R. *J. Chem. Phys.* **1984**, *81*, 3684–3690.
(38) Morris, G. M.; Goodsell, D. S.; Halliday, R. S.; Huey, R.; Hart, W. E.; Belew, R. K.; Olson, A. J. *J. Comput. Chem.* **1998**, *19*, 1639–1662.

Statistical analysis of through-space contacts between amino acids showed that a large degree of conformational flexibility exists in the dendrimers even in their energy minimized state resembling a molten globule. Intramolecular backbone-to-backbone hydrogen bonds were found preferentially between residues at topological distances of $i \leftrightarrow i + 2$, $i \leftrightarrow i + 3$, and $i \leftrightarrow i + 4$ as found in β-turns and α-helices, and were more frequent in the higher generation dendrimers. However, the number of hydrogen bonds per residue was too low to allow the formation of stable secondary structure elements (≤0.33 H-bonds per residue in dendrimers vs. 1 in α-helices or β-sheets).

Despite their conformational flexibility, the dendrimers displayed a pair of cationic residues and the nucleophilic histidine at the dendrimer surface at relative distances compatible with substrate binding by salt bridges to the sulfonate group. Upon substrate docking, the "R" dendrimers showed van der Waals contacts between substrate and the outer layers of aromatic amino acids, which is consistent with the observed stronger substrate binding and catalytic proficiency observed at higher generation number in this series. By contrast, the "H" dendrimers interacted almost exclusively at the core residues with little involvement of the outer layers, in agreement with the fact that the catalytic parameters are not strongly affected by the additional dendrimer generations around the core in this series.

It should be noted that the substrate binding poses were only in a very few cases compatible with ester cleavage by the core catalytic histidine residue. The catalytic mechanism probably involves substrate binding followed by conformational equilibration of the complex until a reactive conformation is encountered. The relatively low frequency of catalytically favorable docked poses might indicate that catalytic turnover is limited by conformational flexibility. This suggests that conformationally constrained dendrimers might be best suited to achieve more protein-like functions such as higher catalytic turnovers. Such dendrimers might be based on structural designs leading to a higher number of intramolecular hydrogen bonds per residue, such as those found in proteins.

Clearly our molecular dynamics study of peptide dendrimers benefited largely from the use of the GROMACS program that has been optimized and validated for proteins. The insight gained by this approach might be of general value for other types of dendrimers such as the very frequently used PAMAM and PPI type dendrimers, which are comparable to peptide dendrimers in composition and conformational flexibility, although they usually consist of only one type of monomer.

Acknowledgment. This work was supported financially by the University of Berne, the Swiss National Science Foundation, and the Marie Curie Training Network IBAAC. We thank Kong Thong Nguyen for assistance in docking studies and in using LigPlot.

Supporting Information Available: Details of the topology manipulation kit for generation of dendrimer models, parametrization of the branching units, molecular dynamics, determination of the hydrodynamic radius from the MD model, experimental hydrodynamic radius using PGSE-NMR, distances between catalytic and binding residues, and substrate−dendrimer contacts in docked complexes. This material is available free of charge via the Internet at http://pubs.acs.org.

JO802743C